agronomy

MDPI

Article

Three-Dimensional Spatial Perception of Blueberry Fruits Based on Improved YOLOv11 Network

Kun Zhao *, **Yuhuan Li** and **Zunmin Liu**

School of Mechanical and Automotive Engineering, Qingdao University of Technology, Qingdao 266520, China; 18612897966@163.com (Y.L.); liu_zunmin@163.com (Z.L.)
* Correspondence: zhao_kun@qut.edu.cn

Abstract: The automated harvesting of blueberries using a picking robot places a greater demand on the 3D spatial perception performance, as the robot's grasping mechanism needs to pick blueberry fruits accurately at specific positions and in particular poses. To achieve this goal, this paper presents a method for blueberry detection, 3D spatial localization, and pose estimation using visual perception, which can be deployed on an OAK depth camera. Firstly, a blueberry and calyx scar detection dataset is constructed to train the detection network and evaluate its performance. Secondly, the blueberry and calyx scar detection model based on a lightweight YOLOv11 (the eleventh version of You Only Look Once) network with an improved depth-wise separable convolution (DSC) module is designed, and a 3D coordinate system relative to the camera is established to calculate the 3D pose of the blueberry fruits. Finally, the above detection model is deployed using the OAK depth camera, leveraging its depth estimation module and three-axis gyroscope to obtain the 3D coordinates of the blueberry fruits. The experimental results demonstrate that the method proposed in this paper can accurately identify blueberry fruits at various maturity levels, achieving a detection accuracy of 95.8% mAP50-95, a maximum positioning error of 7.2 mm within 0.5 m, and an average 3D pose error of 19.2 degrees (around 10 degrees at the ideal picking angle) while maintaining a detection frame rate of 13.4 FPS (frames per second) on the OAK depth camera, providing effective picking guidance for the mechanical arm of picking robots.

Keywords: improved YOLOv11; object detection; 3D localization and pose calculation; blueberry picking

check for updates

Academic Editor: Wan-Soo Kim

Received: 1 February 2025
Revised: 18 February 2025
Accepted: 20 February 2025
Published: 22 February 2025

Citation: Zhao, K.; Li, Y.; Liu, Z. Three-Dimensional Spatial Perception of Blueberry Fruits Based on Improved YOLOv11 Network. *Agronomy* **2025**, *15*, 535. https://doi.org/10.3390/agronomy15030535

1. Introduction

The blueberry harvesting cycle is short, and fruit ripening is inconsistent. Manual picking is labor-intensive, inefficient, and costly [1]. Mechanical harvesting allows large-scale harvesting using methods such as shaking or tapping. Although the harvesting efficiency is high, the fruit loss rate is significant, and the cleaning and sorting of the fruits are required in the later stage [2]. Utilizing robots for automated and precise picking has become an effective solution to address these challenges. For picking robots, the priority is to perceive blueberry fruits in the surrounding environment, accurately determine their position in space, and provide data support for the robotic arm to grasp the fruits. Consequently, accurately identifying blueberries is essential for robots to execute precise picking tasks.

With the help of mature object detection frameworks [3,4], research on blueberry perception has been extensive. These studies primarily enhance the blueberry detection performance in the following ways:

(1) By introducing the attention mechanism, the model can learn more detailed and comprehensive representations of blueberry features.

The Convolutional Block Attention Module (CBAM) [5] was introduced to enhance the feature fusion capability of the blueberry detection network [6]. Feng et al. [7] introduced the SE attention module [8] into the YOLOv9 (the ninth version of You Only Look Once) [9] network, whereas Zhai et al. [10] combined the SE module with BiFPN [11] in the YOLOv5 network to enhance the model's attention to relevant blueberry features while reducing the influence of unnecessary information. Gai et al. [12] introduced the Multiplexed Coordinated Attention (MPCA) module in the last layer of the backbone to improve the feature extraction capability during network training. YOLO-BLBE [13] consisted of the GhostNet [14] module embedded with the Coordinate Attention (CA) mechanism [15] to replace the backbone of YOLOv5s. Yang et al. [16] designed an NCBAM module in the YOLOv5 network, which improved the blueberry feature extraction capability of the backbone network. Liu et al. [17] replaced the C3 module with the Multi-Head Self-Attention (MHSA) module [18] before the SPPF module, enabling the network to learn more comprehensive feature representations and enhancing its understanding of complex spatial relationships and contextual information in blueberry images.

(2) The real-time performance of the detection network is improved by introducing a lightweight convolution module into the network.

The real-time perception of picking robots is crucial to harvesting efficiency. Researchers have developed rapid blueberry detection approaches through the structural optimization of detection networks. Xiao et al. [6] introduced the ShuffleNet [19] module, whereas Yang et al. [16] proposed the C3Ghost module, and Wang et al. [13] introduced the GhostNet [14] module in the YOLOv5 networks. Feng et al. [7] introduced the SC-Conv [20] module in the YOLOv9c network. These lightweight convolution modules significantly reduced the computational complexity of the detection network, which was particularly advantageous for deploying detection models on terminal devices with limited computing resources.

(3) Improving the detection capability of small-scale berry fruits.

The small scale has always been one of the challenges in berry fruit detection [21]. A small object detection layer was introduced to improve the multi-scale recognition capability of blueberries [16]. Liu et al. [17] eliminated the maximum object detection layer from the backbone and head of the network to enhance the model's detection capacity for small-scale blueberry fruits. In addition, researchers have also proposed some small object detection methods for other fruits. Gai et al. [22] proposed a YOLOv4 deep learning algorithm combined with DenseNet [23] to detect cherry fruits, which is more suitable for the recognition of smaller cherry fruits. OrangeYolo [24] contained a channel attention and spatial attention multiscale fusion module to fuse the semantic features of the deep network with the shallow textural detail features, enabling multiscale orange detection. In GHFormerNet [25], a gradient harmonizing classification loss (GHM-R Loss) and a gradient harmonizing regression loss (GHM-R Loss) were introduced to adapt to small apple/begonia fruit detection in the night environment. Similar to reference [16], SM-YOLOv5 [26] introduced a small-target detection layer in the detection network to improve the accuracy of small-target detection for tomatoes.

(4) Addressing occlusion issues.

TL-YOLOv8 [12] proposed the Multi-Scale Separation and Occlusion-Aware Module (MultiSEAM) in the network. The multi-scale separation module captured the multi-scale features of blueberries by segmenting the input image at different scales, while the occlusion-aware module could infer the possible shape and position of the occluded part by analyzing the features of the surrounding area of the blueberry fruits. Feng et al. [7] introduced the MDPIoU loss function [27] to enhance the accuracy of the blueberry detection network in occluded environments.

Although the detection performance of the methods mentioned above was evaluated on private datasets, which cannot be compared horizontally, the results indicate that their detection accuracy can exceed 80%, and some can even exceed 95%, which can guide robotic arms in picking blueberry fruits. However, compared to other fruits, blueberry fruits have a unique characteristic: their skin is thin, which makes them prone to damage during picking. Particularly in the early stages of blueberry fruit ripening, the connection between the fruit stem and the fruit is quite strong, and grasping fruits directly can easily tear the skin. To avoid this problem, experienced pickers commonly hold the plane perpendicular to the fruit axis and rotate it to detach from the fruit stem. Therefore, when the robotic arm's picking mechanism picks fruits according to the above pose and action, relying solely on the 3D spatial position of fruits without considering spatial pose is no longer sufficient to satisfy the needs of precise picking by the robotic arm.

Currently, research on the 3D pose perception of fruits is still limited. Li et al. [28] calculated the symmetry axis using the symmetry plane in the point cloud information of fruits and then evaluated the pose of the fruit in 3D space through the symmetry axis. Christopher Lehnert et al. [29] fitted a hyperelliptic model onto segmented sweet peppers and used nonlinear least squares optimization to estimate the 6DOF pose of the sweet peppers. Lin et al. [30] estimated the 3D pose of a pomegranate fruit by determining its center position and the nearest branch information. Zhang et al. [31] extracted the contours of clustered fruit stems through morphological segmentation, and then employed multidimensional vectors along with Gaussian mixture models to extract the poses of fruit stems. Yun et al. [32] proposed a method to determine the 3D pose of a pomelo by analyzing its boundary shape and applying projection geometry principles using binocular stereovision technology.

The above research on fruit pose estimation is achieved by exploring the characteristics of the fruit, such as symmetry axis, regular contour, position of fruit stem, and the nearest branch to the fruit. These schemes can also be applied to the research of blueberry pose estimation. Therefore, inspired by reference [28] and reference [31], combined with the visual characteristics of blueberry fruit, this paper proposes a blueberry detection, 3D spatial localization, and pose estimation method using visual perception, which can be deployed on an OAK depth camera.

As shown in Figure 1, this method employs an improved lightweight YOLOv11 network to detect blueberry fruits and their calyx scars from the color image. Next, a 3D coordinate system is established based on the image plane, and the 3D pose of every blueberry fruit is calculated using the pixel coordinates of the fruit center and calyx scar center. Then, the depth estimation module in the OAK depth camera (Wuhan Jingtian Electric Appliance Co., Ltd, Wuhan, China) is used to gather the environmental depth information, which is combined with the sensing data from the three-axis gyroscope to calculate the 3D coordinates of each blueberry fruit relative to the camera. Finally, the 3D spatial position and pose information of blueberry fruits obtained through this method can be transmitted to the subsequent picking decision and control system.

The remainder of the work is organized as follows. In Section 2, the blueberry and calyx scar detection method is described, including the blueberry and calyx scar dataset and the improved lightweight YOLOv11 detection network. In addition, Section 2 also introduces the 3D spatial localization and pose calculation method for blueberry fruits, based on the detection results of blueberries and calyx scars. The experimental results are given in Section 3, and the work is summarized in Section 4.

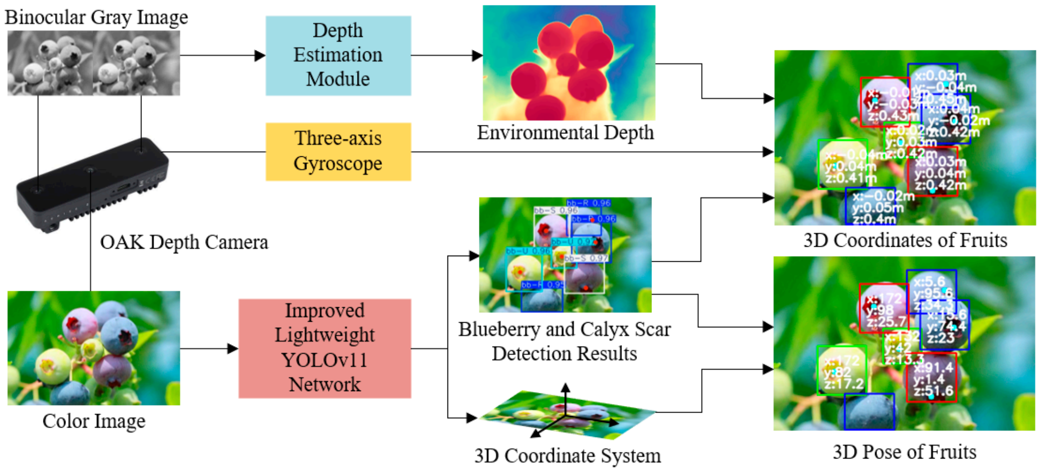

Figure 1. Schematic diagram of blueberry 3D spatial localization and pose calculation.

2. Materials and Methods

2.1. Blueberry and Calyx Scar Detection Dataset

2.1.1. Collection and Partition of Blueberry Images

This paper primarily employs three ways to collect blueberry images. The first way is to take live-action shots at the Wolin Blueberry Base in Qingdao, Shandong, China, obtaining 642 original blueberry images under different harvesting conditions, such as sunny, cloudy, backlit, occlusion, denseness, and sparseness, as shown in Figure 2. The second way is to capture online images using web crawling technology, obtaining 1358 images. The third way involves data augmentation of 1500 images collected through the first two ways, generating 3000 images, including translation, flipping, rotation, brightness adjustment, and adding white noise. The partial augmentation is shown in Figure 3.

The dataset, which contains 5000 blueberry images collected through the above three ways, is divided into the training set, validation set, and testing set in an 8:1:1 ratio for detection network training and performance testing. It should be noted that data augmentation can lead to correlations between data. To avoid overfitting in the trained detection network, all 500 samples in the testing set are only the original images that have not undergone data augmentation.

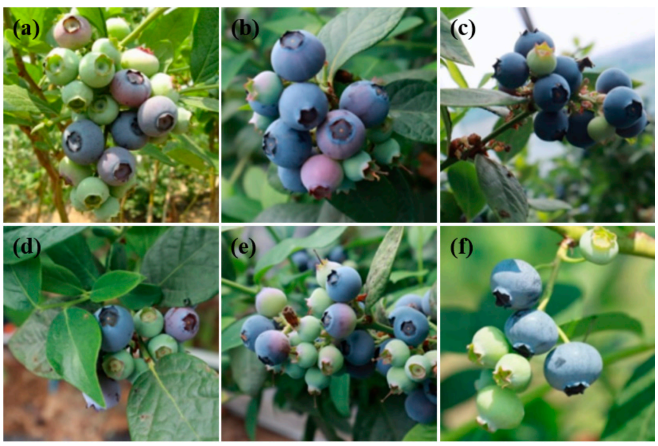

Figure 2. Schematic diagram of blueberry images under different harvesting conditions: (**a**) sunny, (**b**) cloudy, (**c**) backlit, (**d**) occlusion, (**e**) denseness, (**f**) sparseness.

Figure 3. Schematic diagram of partial data augmentation: (**a**) original image, (**b**) rotation, (**c**) brightness adjustment, (**d**) white noise.

2.1.2. Data Annotations

This paper uses manual annotation software called LabelMe (Version 4.5.13) to complete the data labeling task. This software can generate a JSON file containing the image name, size, position, and specific annotation information for each image. During the annotation process, the blueberry fruits are roughly divided into three categories based on maturity: ripe blueberries, semi-ripe blueberries, and unripe blueberries, with RGB colors corresponding to purple red, light red, and cyan, respectively.

The axis information of the blueberry fruit in the image can reflect its 3D pose, which can be determined by connecting the stem or calyx scar center to the fruit center. For clustered blueberries, it is more convenient to detect the calyx scar as their visibility is stronger than that of the fruit stem. Therefore, to obtain the fruit pose, the calyx scar centers of the blueberry fruits are also marked with dots, as shown in Figure 4. Finally, the annotation information of blueberry and calyx scar converted to YOLO format can be represented as follows:

$$Lable = \left[cls, c_x, c_y, w, h, kp_x, kp_y, vis\right], \tag{1}$$

where *cls* represents the blueberry maturity categories, and 'bb_R', 'bb_S', and 'bb_U' represent the three states of the blueberry: ripe, semi-ripe, and unripe, respectively; c_x and c_y represent the center coordinates of the bounding box, and w and h represent the length and width of the bounding box. kp_x and kp_y represent the coordinates of the calyx scar center; *vis* represents the visibility of the calyx scar center, 'zero' is visible, and 'two' is invisible. When the calyx scar center is invisible, the values of kp_x and kp_y are both 'zero'.

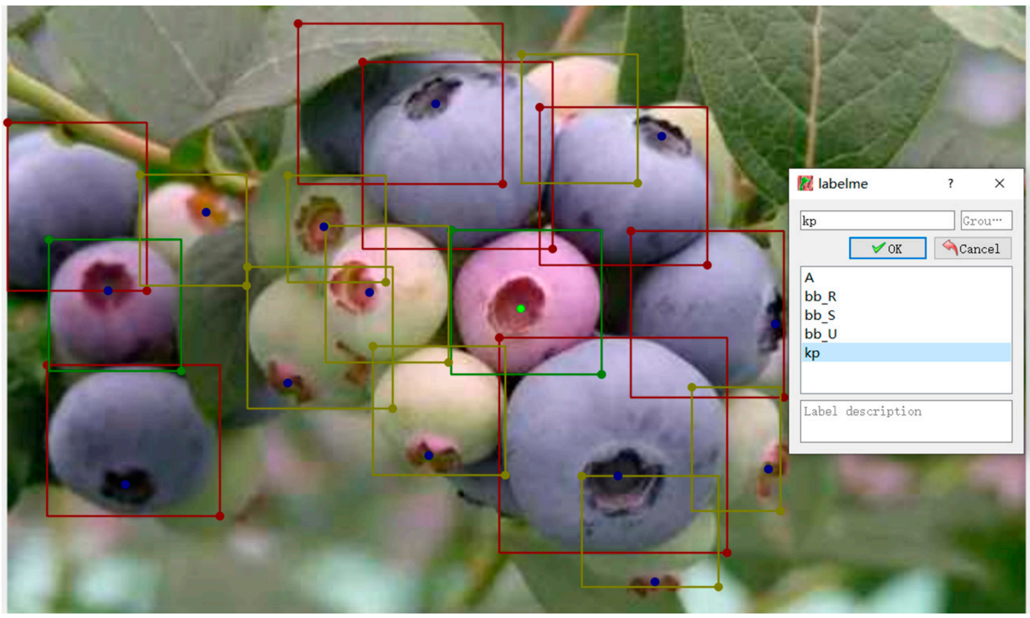

Figure 4. Schematic diagram of blueberries and calyx scar annotation.

Blueberries grow in clusters and have many individual fruits, making annotation time-consuming and laborious. To reduce workload, this paper divides the annotation into three stages. In the first stage, 500 images are labeled, and a preliminary model for blueberry and calyx scar detection is trained based on the YOLO network. In the second stage, the trained model is used to detect other unlabeled blueberry images, and the detection results are converted into JSON format as prelabeled information. In the last stage, the inaccurate prelabeled results are refined to generate accurate labeling information in LabelMe and finally converted into annotation files that are readable by YOLO.

2.2. Blueberry and Calyx Scar Detection Network

When utilizing a robot for blueberry picking, it is crucial to improve the picking efficiency. The YOLO series networks represent a seminal real-time detection framework in the object detection field, renowned for its exceptional detection accuracy coupled with minimal computational overhead, making it a ubiquitous choice for a wide array of embedded devices. The YOLO series networks currently have 11 versions and have spawned multiple variants based on them. Among them, YOLOv10 [33] and YOLOv11 [34] adopt the consistent dual assignments strategy, significantly reducing computational overhead and meeting the requirements of blueberry detection.

2.2.1. Basic Structure of the YOLOv11n Network

As shown in Figure 5, the YOLOv11n network consists of three parts: Backbone, Neck, and Head. Backbone gradually extracts high-order features of the target by stacking CBS, C3k2, SPPF, and C2PSA modules. Neck uses modules such as Upsample, C3k2, and CBS to construct a convolutional pyramid, and mixes the shallow features extracted by Backbone to enable the network to learn the salient features of the targets. In addition, Neck adopts a multi-scale output strategy to obtain three feature layers with different scales to meet the needs of multi-scale object detection. Head consists of two branches: one2many and one2one, used for NMS-Free training and inference [33]. The structure of Head varies depending on different visual tasks such as object detection, pose detection, and instance segmentation.

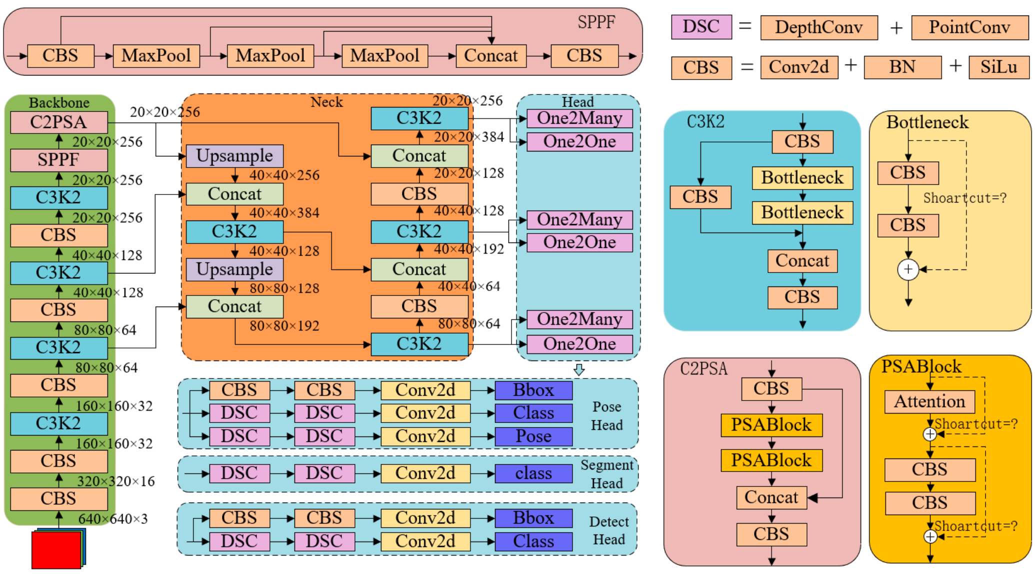

Figure 5. Schematic diagram of the YOLOv11n network framework. The three-dimensional numbers represent the width scale, the height scale, and the channel number of the feature layers, respectively.

2.2.2. Improved Lightweight YOLOv11 Network for Blueberry and Calyx Scar Detection

Although the YOLOv11 is designed with different parameter scales to adapt to perception tasks of varying complexity, the parameters of YOLOv11 are still redundant for blueberry detection due to the low diversity of fruit shape (i.e., circular or elliptical) and color (i.e., cyan, red, or purple). Therefore, considering the unique characteristics and requirements for blueberry detection, this paper designs a lightweight network to maximize the detection accuracy and efficiency based on the YOLOv11 framework. The specific network structure is shown in Figure 6.

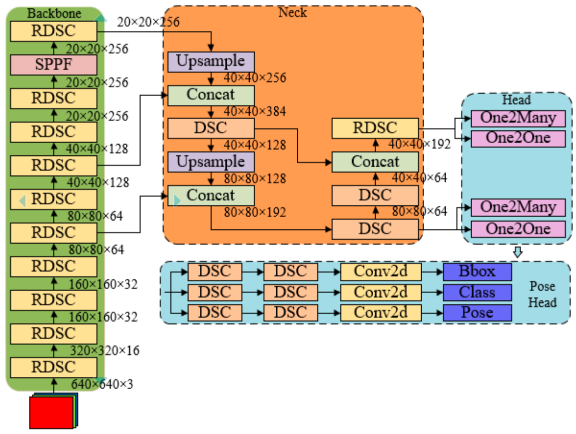

Figure 6. Schematic diagram of blueberry and calyx scar detection network framework.

Comparing Figures 5 and 6, this paper made improvements in the following aspects of blueberry and calyx scar detection:

- Proposing an improved depth-wise separable convolution (DSC) module with DSC and reverse DSC to replace the CBS and C3K2 modules.

As shown in Figure 7a, the DSC module [35] decomposes the traditional convolution into two sequential processes: depth-wise convolution and point-wise convolution. Depth-wise convolution extracts spatial information from each feature channel independently, and point-wise convolution mixes features between channels, significantly reducing network computation while sacrificing some model performance.

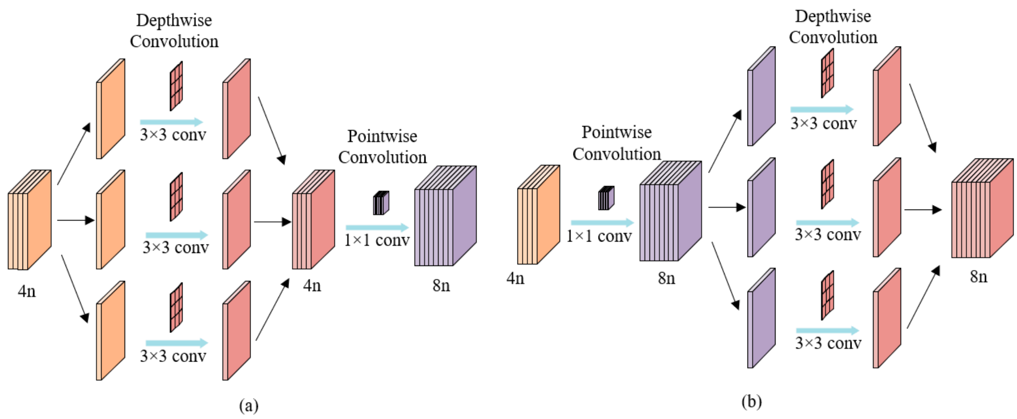

Figure 7. Schematic diagram of improved DSC module: (**a**) DSC module, (**b**) reverse DSC module.

Subsequent experimental results show that directly using the DSC module instead of the convolution module in YOLOv11 will significantly decrease the accuracy of blueberry and calyx scar detection. By analyzing the structure and parameter characteristics of the detection network in Figure 6, it is discovered that the convolution process generally involves an increase or decrease in feature dimensionality. The order of depth-wise convolution and point-wise convolution will affect the ability of each layer to extract blueberry spatial features and the computational complexity of the network. As shown in Figure 7a, the feature dimension increases from *4n* to *8n*. However, influenced by the order of depth-wise convolution and point-wise convolution, the number of spatial features extracted by the DSC module is only *4n*, which is insufficient to learn the spatial features of blueberry fruits well.

Therefore, this paper proposes an improved DSC module that can adaptively change the order of depth-wise convolution and point-wise convolution based on whether the feature dimension is increased or decreased. When the feature dimension increases, the reverse DSC (RDSC) depicted in Figure 7b is employed to extract features; conversely, the DSC illustrated in Figure 7a is utilized, ensuring that the network is capable of learning more spatial features of blueberries.

- Removing the attention mechanism module C2PSA at the end of the Backbone network.

The experiments showed that the attention mechanism module C2PSA did not significantly improve the performance of blueberry detection, but instead produced inefficient computations. Therefore, it was removed from the detection network proposed in this paper.

- Retaining only the relatively large-scale outputs of features with 80 × 80 pixels and 40 × 40 pixels.

Given the comparatively small scale of the blueberry fruits in the image, the detection head only outputs detection results at the larger scales of 80 × 80 pixels and 40 × 40 pixels. This diminishes computational complexity and prompts the model to be more apt at learning the detailed features of blueberries, such as the details around the calyx scar.

2.3. Three-Dimensional Spatial Localization and Pose Calculation of Blueberry Fruits

2.3.1. Three-Dimensional Pose Calculation

During blueberry picking, the gripper mechanism must grasp the blueberry fruit in a plane roughly perpendicular to its axis, and then rotate the fruit around this axis to detach it from the stem, preventing damage to the fruit's skin. Clarifying the fruit pose in 3D space is a prerequisite for achieving the above operation.

Assuming the camera is installed at the end of the robotic arm, that is, the camera follows the movement of the robotic arm, the ideal picking pose of the fruit in the image should be as shown in Figure 8. That is, the fruit is located at the center of the image, and its axis is approximately perpendicular to the image plane. Therefore, this study establishes a 3D coordinate system with the image plane as a reference. This coordinate system takes the image center as the origin, the image plane as the XY plane, and the direction perpendicular to the image plane as the Z-axis.

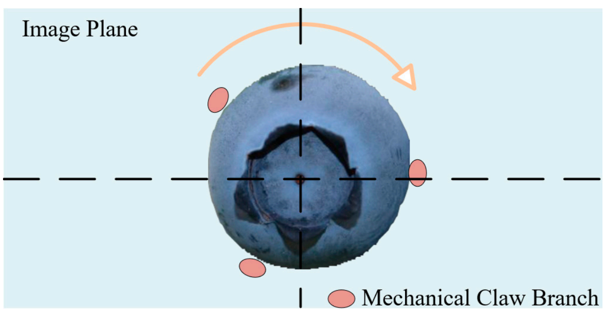

Figure 8. Ideal picking pose of blueberry fruit in the image.

As shown in Figure 9, the fruit pose can be calculated based on the results of blueberry and calyx scar detection. The required data include the height and width of the bounding box, the center coordinates of the fruit, and the center coordinates of the calyx scar. The calculation formula for the blueberry fruits' 3D pose is as follows:

$$Pose_{3D} = \begin{cases} \theta_x = arccos(\frac{\triangle x}{l}) \\ \theta_y = arccos(\frac{\triangle y}{l}) \\ \theta_z = arcsin(\frac{l}{r}) \end{cases} \tag{2}$$

where l is the distance between the fruit center and the calyx scar center, and its extension line is also the fruit axis; Δx and Δy are the components of distance l on the X-axis and Y-axis; r is the fruit radius; and θ_x, θ_y, and θ_z are the angles between the fruit axis and the XYZ axes. Due to the shape of blueberry fruits being mostly circular or elliptical in the image plane, the fruit radius r is approximately calculated using the width B_w and height B_h of the bounding box. Note that this is only valid for fruits with regular shapes.

From Figure 9 and Equation (2), it can be seen that the smaller the pixel distance l, the smaller the angle between the fruit axis and the Z-axis, which is closer to the ideal picking pose of the blueberry fruit.

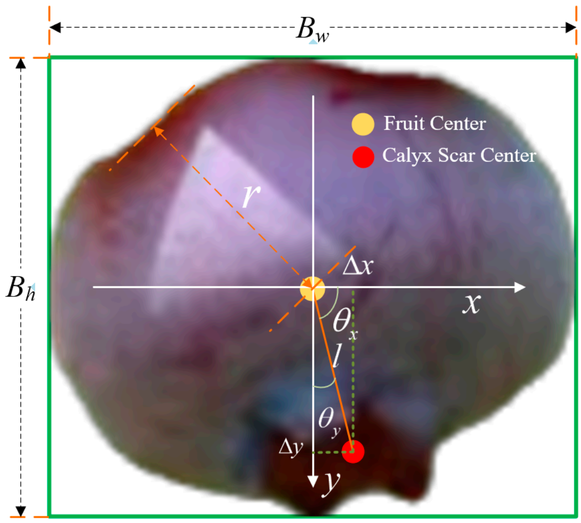

Figure 9. Schematic diagram of 3D pose calculation of blueberry fruits.

2.3.2. Three-Dimensional Spatial Localization

To ensure the precise picking of blueberry fruits by the robotic arm, it is crucial to obtain accurate relative positional information between the gripper mechanism and the fruits. The OAK-D-Pro depth camera used in this paper contains a depth estimation module that can directly obtain environmental depth information. The depth estimation module has two ranging methods, namely, structured light ranging and binocular depth ranging. Through algorithm fusion, the ranging error of the OAK camera within 4 m is less than 2%. The closer the distance, the smaller the ranging error, meeting the requirements for blueberry picking. By combining the depth information, the blueberry detection results, and the sensor data from BMI270 three-axis gyroscopes, the 3D coordinate of each fruit relative to the OAK camera can be ascertained.

In this way, by obtaining the 3D spatial position and pose of blueberry fruits, the robotic arm electronic control system can guide the gripper mechanism to reach the designated position and perform precise picking operations according to specific poses and actions.

3. Results and Discussion

The experiment in this paper is divided into three stages. The first stage is to construct and train a blueberry and calyx scar detection model based on the deep learning framework

PyTorch (Version 2.1.2), which can obtain the detection results of blueberry fruit and calyx scar center on the image plane in the form of rectangular boxes and key points, respectively. The detection performance of models with different parameter scales and modules is compared, and some detection results are visualized. The second stage is to calculate the 3D pose information of blueberry fruits on the constructed 3D coordinate system based on the detection results of the first stage. The errors of pose estimation in three directions are evaluated and analyzed. In the third stage, the trained detection model is converted into blob format and deployed to the OAK depth camera. It can detect blueberry fruits on terminal devices and obtain the 3D coordinates of blueberry fruits relative to the depth camera with the help of its internal depth estimation module. Whether the positioning error meets the requirements under the blueberry picking task is analyzed.

3.1. Blueberry and Calyx Scar Detection Results

3.1.1. Experimental Result Statistics

As shown in Table 1, on the blueberry and calyx scar detection dataset, the proposed method can achieve an accuracy of 99.2% mAP50 and 95.8% mAP50-90 for blueberry detection, as well as an accuracy of 87.0% mAP50 and 86.6% mAP50-90 for calyx scar detection. The time taken for the proposed model to detect a 640 × 640-pixel image on the NVIDIA GeForce GTX 4090 and 13900KF CPU is 0.4 ms, making it suitable for picking robots that require fast and precise blueberry detection. Furthermore, Table 1 also displays the specific performance of blueberry detection at three maturity levels, which shows that the blueberry detection accuracy at all maturity levels is very high.

Table 1. Detection results for blueberry and calyx scar testing set.

Category	Blueberry Detection		Calyx Scar Detection		Time Consumption (ms)
	mAP50 (%)	mAP50-95 (%)	mAP50 (%)	mAP50-95 (%)	
All	99.2	95.8	87.0	86.6	0.4
bb_R	99.5	96.2	87.2	86.8	
bb_S	99.1	94.9	85.4	84.9	
bb_U	99.0	96.2	88.3	88.2	

In addition, some ablation experiments are presented, which evaluate the detection performance of the DSC, improved DSC (ours), and CBS modules within the YOLO framework across three parameter scales: N, S, and M. For detailed parameters, please refer to the description of YOLOv11.

Table 2 shows that all models can achieve over 93.5% mAP50-90 for blueberry detection, which meets the demand for blueberry picking. For calyx scar detection, the mAP50-95s of all models are relatively low, only around 84.1% to 88.2%. Specifically, the models with the M scale do not improve detection performance compared to models with the S scale, but increase the models' time consumption significantly. Therefore, these models with the M scale are unsuitable for blueberry and calyx scar detection. At the N and S scales, models with DSC modules have the fastest detection speed, but their detection accuracies are only 84.1% and 85.2% mAP50-95. The detection accuracies of models with the improved DSC modules are slightly lower than models with the CBS modules, at 0.7% and 0.3% mAP50-95, respectively, but their detection speeds are faster. It can be seen that the improved DSC module proposed in this paper significantly improves detection speed while slightly sacrificing detection accuracy. It is worth noting that the accuracy of calyx scar detection is significantly lower than that of fruit detection. This gap will propagate errors to attitude estimation of blueberry fruits.

For the blueberry picking task, detection speed is more important than detection accuracy, because missed or obstructed blueberries will become detected blueberries as the viewing angle changes during the continuous picking process. Therefore, this paper selects the model with the improved DSC module at the N scale as the blueberry and calyx scar detection model.

Table 2. Performance comparison of detection models with different parameter scales and modules.

Para. Scale	Module	Blueberry Detection		Calyx Scar Detection		Time Consumption (ms)
		mAP50-95 (%)	Improvement (%)	mAP50-95 (%)	Improvement (%)	
N	DSC	93.5	base	84.1	base	0.3
	Ours	95.8	+2.3	86.6	+2.5	0.4
	CBS	96.2	+2.7	87.3	+3.2	0.6
S	DSC	93.8	+0.3	85.2	+1.1	0.4
	Ours	96.0	+2.5	87.7	+3.6	0.5
	CBS	96.3	+2.8	88.0	+3.9	0.8
M	DSC	93.9	+0.4	84.9	+0.8	1.6
	Ours	96.1	+2.6	87.5	+3.4	1.8
	CBS	96.4	+2.9	88.2	+4.1	2.1

3.1.2. Visualization of Detection Instances

To verify the practicality of the proposed detection network, some blueberry images were selected from the testing set for the visual representation of the detection results, as shown in Figure 10. As can be seen, the proposed detection network can accurately identify blueberry fruits of different maturity levels, which is beneficial for picking only ripe blueberries and reducing fruit damage rates. At the same time, the point detection of the calyx scar is also basically accurate, which is beneficial for the 3D pose calculation of blueberry fruits. However, it can also be seen that the bounding box regression error of some fruit individuals, such as the leftmost in the middle image below, is relatively large. This is related to the occlusion and small scale of the fruits, as the detection accuracy is mainly lost in detecting these difficult objects.

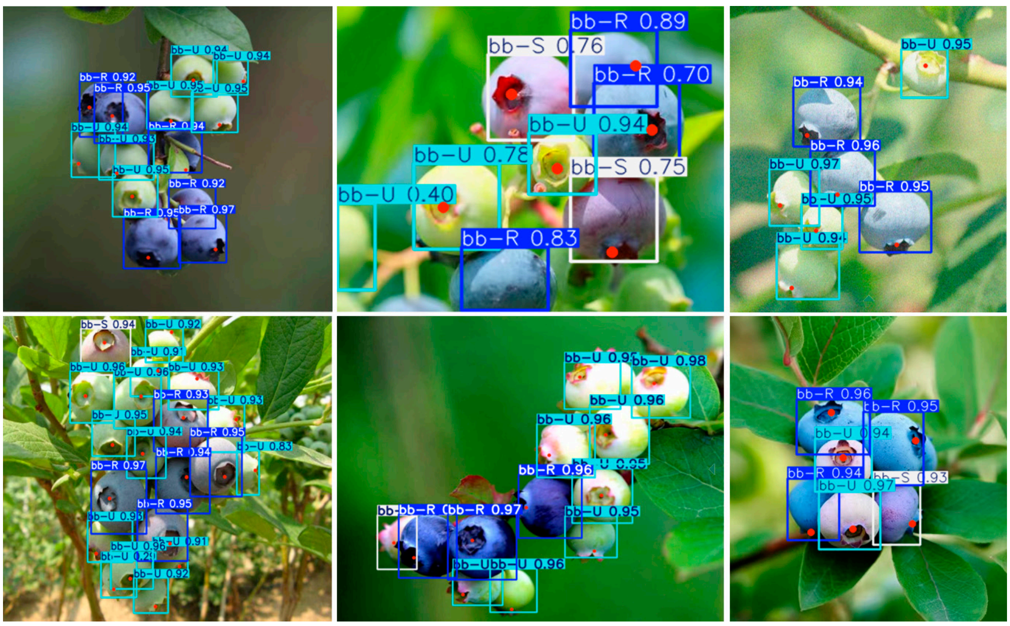

Figure 10. Visualization of blueberry and calyx scar detection results. The numbers in the figure represent the confidence of predicting blueberry categories, with a value range of 0–1. The red dots indicate the predicted center of the calyx scar.

3.2. Three-Dimensional Pose Calculation Results for Blueberry Fruits

According to the calculation in Section 2.3.1, the 3D poses of blueberry fruits are shown in Figure 11. It should be noted that the 3D poses of blueberry fruits with invisible calyx scars are not displayed.

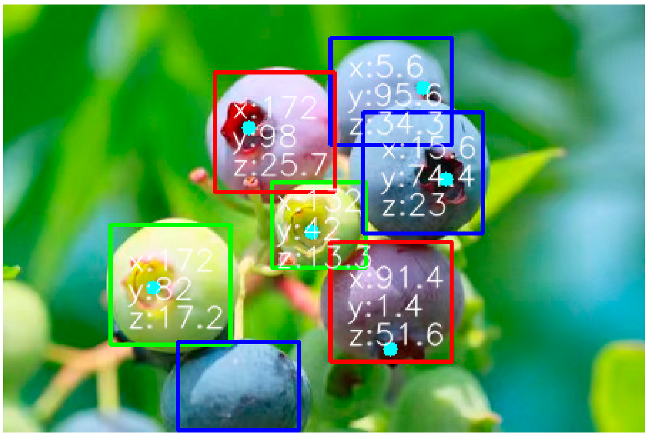

Figure 11. Three-dimensional poses of blueberry fruits.

Based on the recorded detection results of blueberries and calyx scars in the testing set compared with the ground truth, we calculated the average error of the predicted 3D pose estimation of networks with different modules in three directions. The statistical results are shown in Table 3.

Table 3. Average errors of pose estimation of networks with different modules in three directions.

Module	Average Errors (°)		
	X-Axis	Y-Axis	Z-Axis
DSC	16.4	17.6	23.7
Ours	13.7	14.2	19.2
CBS	13.3	14.4	18.6

It can be seen that the average error of pose estimation of the detection network proposed in this paper is significantly lower than that of the network with the DSC module, only slightly higher than that of the network with the CBS module, and slightly lower in the Y-axis direction. We analyzed some of the blueberry and calyx scar detection results and the pose estimation results calculated from them, and found that there was a double-negative compensation effect, which enabled relatively accurate posture estimation results to be obtained even if there were significant errors in the detection results. Therefore, for some individual fruits, the errors in blueberry and calyx scar detection may not necessarily amplify the pose estimation errors calculated from the detection results.

In fact, the picking robot is more concerned with the prediction error of the fruit axis in the Z-axis direction (i.e., perpendicular to the image plane), as it determines whether the fruit is in the ideal picking pose. In Table 3, it can be seen that the average error in the Z-axis direction is slightly higher than that in the X-axis and Y-axis directions. In Equation (2), the calculation error of the angle between the fruit axis and the Z-axis is related to the errors of the fruit radius and the distance from the calyx scar center to the fruit center. Therefore, the reasons for the above phenomenon include three aspects: (1) The regression error of bounding boxes of some individual fruits is relatively large, which directly affects the accuracy of the fruit radius and center coordinates. (2) The detection accuracy of calyx scars is significantly lower than that of fruit, and this error is transmitted to the calculation error of the pose estimation. (3) Even if the bounding box regression and calyx scar center detection are accurate, the approximate error in calculating the fruit radius using the length and width information of the bounding boxes will amplify the calculation error of the angle between the fruit axis and the Z-axis.

To quantify whether the pose estimation errors in the Z-axis direction meet the requirements of the picking robot, we conducted a detailed analysis of the errors and calculated the errors at different angles of the fruit axis (every 5 degrees). The statistical results are shown in Figure 12. It can be seen that the angle between the fruit axis and the Z-axis is smaller, the error of the prediction angle is also smaller, and, conversely, the error is larger. Therefore, during the picking process, as the robotic arm moves, the angle between the fruit axis and the Z-axis will become smaller, and the prediction error will also become smaller, eventually converging to a smaller angle range (approximately 10 degrees). This is sufficient to meet the picking action requirement of the grasping mechanism, that is, to twist the fruit around the approximate axis of the fruit so that it can be separated from the stem without damage.

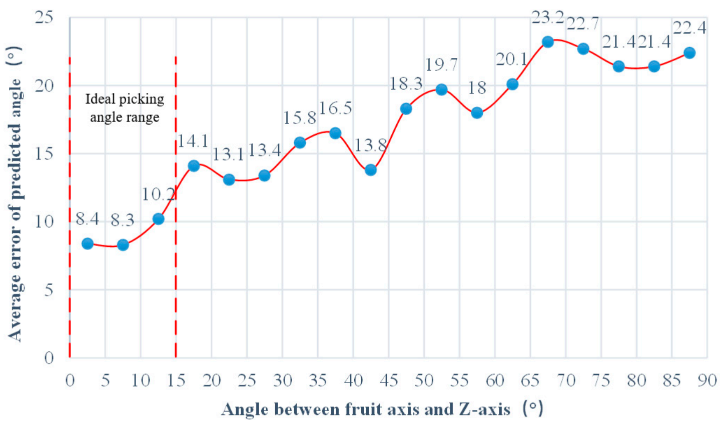

Figure 12. Error statistics of fruit axis within different angle ranges in the Z-axis direction.

3.3. Three-Dimensional Localization Results for Blueberry Fruits

The blueberry and calyx scar detection model trained on the server is a pt file. Through the official tutorial provided by OAKChina, in this study, we converted the pt file into the blob format supported by the OAK depth camera. The OAK camera can directly locate the 3D coordinates of the detected blueberry fruits by using the internal depth estimation module. A schematic diagram of the environmental depth estimation and blueberry fruit localization is shown in Figure 13.

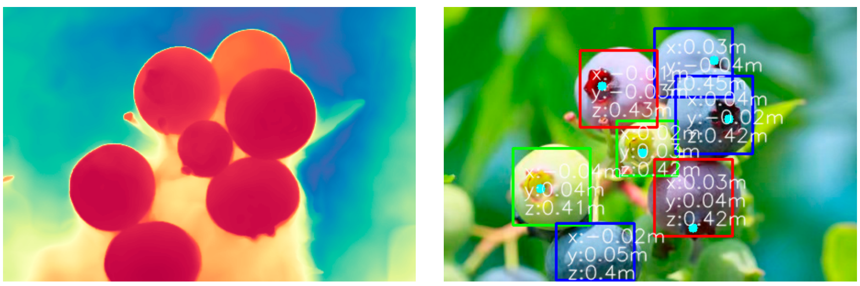

(**a**) (**b**)

Figure 13. Environmental depth estimation (**a**) and 3D coordinates of blueberry fruits (**b**).

In order to verify the positioning accuracy of the OAK camera, a total station (Topcon Sojia (Shanghai) Technology and Trade Co., Ltd, Shanghai, China) was used to measure the coordinates of 100 points within a range of 0.5 m from the OAK camera. These groundtruths were compared with the predicted coordinates provided by the OAK camera to calculate the positioning error. Statistics show that the average error is 3.9 mm, and the maximum error is 7.2 mm. This is consistent with the technical parameters (less than 2% within 4 m) provided by the supplier of OAK cameras. Therefore, the positioning accuracy of the OAK camera is considered to satisfy the precise perception requirements for robotic arms.

The perception model with the improved DSC module deployed on the OAK depth camera can achieve a detection speed of 13.4 FPS (frames per second), while the model with the CBS module has a detection speed of only 9.3 FPS. Therefore, the proposed detection model can better satisfy the requirements of terminal devices for detection efficiency.

3.4. Discussion

Through the analysis of the above experiments and results, it can be concluded that the proposed blueberry 3D spatial perception method has good performance and can be applied to the perception system of blueberry-picking robots. However, there are still several issues that need to be considered.

(1) The performance of the detection network needs further improvement, especially the detection accuracy of the calyx scar. This may require increasing the sample number of the dataset or further optimizing the structure of the detection network. In addition, many of the calyx scar centers are invisible, making it impossible to calculate the pose of the fruit in subsequent processing. Detecting the corresponding fruit stem may be a supplementary method.

(2) The calculation of fruit radius is based on the assumption that the shape of blueberries is approximately circular. For blueberry varieties with other shapes, this approximation error will be transmitted to the pose estimation. By using ellipses instead of bounding boxes, the contour of the fruit can be better fitted, and then the calculation of the major axis of the ellipse as the diameter of the fruit will be more accurate.

(3) In the real world, some variable factors such as the continuous movement of fruits caused by wind and changes in lighting can affect the perception accuracy and subsequent picking. In order to ensure that the real-time detection can counteract the impact of fruit position change (assuming it is 1 cm) caused by branch shaking on picking, the movement speed of the fruit should not exceed 0.14 m/s, which is related to factors such as the strength of the wind and of the branches. A more effective way is to use the robotic arm to grab branches to fix the blueberry fruits. For the impact of lighting changes, the dataset will supplement more samples under different lighting conditions to make the detection model more robust.

(4) The size of the dataset needs to be expanded to improve detection performance, including static images and synthetic images, and a further increase in sample number is needed in the future.

4. Conclusions

To satisfy the demand for automated and precise blueberry picking operations, this paper proposes a blueberry fruit detection, 3D spatial localization, and pose calculation method using visual perception. The improved lightweight YOLOv11 model proposed in this paper can perceive blueberry fruits and calyx scars of different maturity levels in images and calculate the 3D pose information of blueberry fruits relative to the camera. The detection model, used with the OAK camera, can use its internal depth estimation module and the three-axis gyroscope to obtain the 3D coordinates of blueberry fruits. The experimental results show that the blueberry identification method can achieve a detection accuracy of 95.2% mAP50-95 for blueberry fruits. The 3D positioning error of blueberry fruits can be controlled within 1 cm within a range of 0.5 m, and the 3D pose estimation error can be controlled within 19.2 degrees. This performance can fulfill the requirement for 3D spatial perception of blueberries during automated and precise picking operations by robotic arms. Therefore, the research in this paper is of great significance for improving the blueberry picking efficiency and reducing picking costs and fruit damage rates, thus exhibiting extensive application potential.

Author Contributions: Conceptualization, K.Z. and Y.L.; methodology, K.Z.; software, K.Z.; validation, K.Z., Y.L. and Z.L.; investigation, K.Z.; resources, Y.L. and Z.L.; data curation, K.Z. and Y.L.; writing—original draft preparation, K.Z.; writing—review and editing, K.Z., Y.L. and Z.L.; visualization, K.Z.; supervision, K.Z.; project administration, Y.L. All authors have read and agreed to the published version of the manuscript.

Funding: This research was supported by the Shandong Provincial Natural Science Foundation (No. ZR2022QE231).

Data Availability Statement: The datasets presented in this article are not readily available because the data are part of an ongoing study. Requests to access the datasets should be directed to the corresponding author (e-mail address: zhao_kun@qut.edu.cn).

Conflicts of Interest: The authors declare no conflicts of interest.

References

1. Lobos, G.A.; Bravo, C.; Valdés, M.; Graell, J.; Ayala, I.L.; Beaudry, R.M.; Moggia, C. Within-plant variability in blueberry (*Vaccinium corymbosum* L.): Maturity at harvest and position within the canopy influence fruit firmness at harvest and postharvest. *Postharvest Biol. Tec.* **2018**, *146*, 26–35. [CrossRef]
2. Brondino, L.; Briano, R.; Massaglia, S.; Giuggioli, N.R. Influence of harvest method on the quality and storage of highbush blueberry. *J. Agric. Food Res.* **2022**, *10*, 100415–100423. [CrossRef]
3. Redmon, J.; Divvala, S.; Girshick, R.; Farhadi, A. You Only Look Once: Unified, real-time object detection. In Proceedings of the 2016 IEEE/CVF Conference on Computer Vision and Pattern Recognition (CVPR 2016), Las Vegas, NV, USA, 27–30 June 2016.
4. Ren, S.; He, K.; Girshick, R.; Sun, J. Faster R-CNN: Towards real-time object detection with region proposal networks. *IEEE Trans. Pattern Anal. Mach. Intell.* **2017**, *39*, 1137–1149. [CrossRef] [PubMed]
5. Woo, S.; Park, J.; Lee, J.Y.; Kweon, I.S. CBAM: Convolutional block attention module. In Proceedings of the 15th European Conference on Computer Vision (ECCV 2018), Munich, Germany, 8–14 September 2018.
6. Xiao, F.; Wang, H.; Xu, Y.; Shi, Z. A Lightweight Detection Method for Blueberry Fruit Maturity Based on an Improved YOLOv5 Algorithm. *Agriculture* **2024**, *14*, 36. [CrossRef]
7. Feng, W.; Liu, M.; Sun, Y.; Wang, S.; Wang, J. The use of a blueberry ripeness detection model in dense occlusion scenarios based on the improved YOLOv9. *Agronomy* **2024**, *14*, 1860. [CrossRef]
8. Hu, J.; Shen, L.; Sun, G. Squeeze-and-excitation networks. In Proceedings of the 2018 IEEE/CVF Conference on Computer Vision and Pattern Recognition (CVPR 2018), Salt Lake City, UT, USA, 18–22 June 2018.
9. Wang, C.Y.; Yeh, I.H.; Mark Liao, H.Y. YOLOv9: Learning what you want to learn using programmable gradient information. In Proceedings of the 18th European Conference on Computer Vision (ECCV 2024), Milan, Italy, 29 September–4 October 2024.
10. Zhai, X.; Zong, Z.; Xuan, K.; Zhang, R.; Shi, W.; Liu, H.; Han, Z.; Luan, T. Detection of maturity and counting of blueberry fruits based on attention mechanism and bi-directional feature pyramid network. *Food Meas.* **2024**, *18*, 6193–6208. [CrossRef]
11. Tan, M.; Pang, R.; Le, Q.V. EfficientDet: Scalable and efficient object detection. In Proceedings of the 2020 IEEE/CVF Conference on Computer Vision and Pattern Recognition (CVPR 2020), Seattle, WA, USA, 14–19 June 2020.
12. Gai, R.; Liu, Y.; Xu, G. TL-YOLOv8: A blueberry fruit detection algorithm based on improved YOLOv8 and Transfer Learning. *IEEE Access* **2024**, *12*, 86378–86390. [CrossRef]
13. Wang, C.; Han, Q.; Li, J.; Li, C.; Zou, X. YOLO-BLBE: A Novel Model for Identifying Blueberry Fruits with Different Maturities Using the I-MSRCR Method. *Agronomy* **2024**, *14*, 658. [CrossRef]
14. Han, K.; Wang, Y.; Tian, Q.; Guo, J.; Xu, C.; Xu, C. GhostNet: More features from cheap operations. In Proceedings of the 2020 IEEE/CVF Conference on Computer Vision and Pattern Recognition (CVPR 2020), Seattle, WA, USA, 14–19 June 2020.
15. Hou, Q.; Zhou, D.; Feng, J. Coordinate attention for efficient mobile network design. In Proceedings of the 20201 IEEE/CVF Conference on Computer Vision and Pattern Recognition (CVPR 2021), Nashville, TN, USA, 20–25 June 2021.
16. Yang, W.; Ma, X.; Hu, W.; Tang, P. Lightweight Blueberry Fruit Recognition Based on Multi-Scale and Attention Fusion NCBAM. *Agronomy* **2022**, *12*, 2354. [CrossRef]

17. Liu, Y.; Zang, W.; Ma, H.; Liu, Y.; Zhang, Y. Lightweight YOLO v5s blueberry detection algorithm based on attention mechanism. *J. Henan Agric. Sci.* **2024**, *53*, 151–157.
18. Vaswani, A.; Shazeer, N.; Parmar, N.; Uszkoreit, J.; Jones, L.; Gomez, A.N.; Kaiser, Ł.; Polosukhin, I. Attention is all you need. In Proceedings of the Advances in Neural Information Processing Systems, Long Beach, CA, USA, 4–9 December 2017.
19. Zhang, X.; Zhou, X.; Lin, M.; Sun, J. ShuffleNet: An extremely efficient convolutional neural network for mobile devices. In Proceedings of the 2018 IEEE/CVF Conference on Computer Vision and Pattern Recognition (CVPR 2018), Salt Lake City, UT, USA, 18–22 June 2018.
20. Li, J.; Wen, Y.; He, L. SCConv: Spatial and channel reconstruction convolution for feature redundancy. In Proceedings of the 2023 IEEE/CVF Conference on Computer Vision and Pattern Recognition (CVPR 2023), Vancouver, BC, Canada, 18–22 June 2023.
21. Wang, C.; Pan, W.; Zou, T.; Li, C.; Han, Q.; Wang, H.; Yang, J.; Zou, X. A Review of Perception Technologies for Berry Fruit-Picking Robots: Advantages, Disadvantages, Challenges, and Prospects. *Agriculture* **2024**, *14*, 1346. [CrossRef]
22. Gai, R.; Chen, N.; Yuan, H. A detection algorithm for cherry fruits based on the improved YOLO-v4 model. *Neural Comput. Appl.* **2023**, *35*, 13895–13906. [CrossRef]
23. Huang, G.; Liu, Z.; Van Der Maaten, L.; Weinberger, K. Densely connected convolutional networks. In Proceedings of the 2017 IEEE/CVF Conference on Computer Vision and Pattern Recognition (CVPR 2017), Honolulu, HI, USA, 21–26 July 2017.
24. Zhang, W.; Wang, J.; Liu, Y.; Chen, K.; Li, H.; Duan, Y.; Wu, W.; Shi, Y.; Guo, W. Deep-learning-based in-field citrus fruit detection and tracking. *Hort. Res.* **2022**, *9*, 1–15. [CrossRef] [PubMed]
25. Sun, M.; Xu, L.; Luo, R.; Lu, Y.; Jia, W. GHFormer-Net: Towards more accurate small green apple/begonia fruit detection in the nighttime. *J. King Saud Univ.-Comput. Inf. Sci.* **2022**, *34*, 4421–4432. [CrossRef]
26. Wang, X.; Wu, Z.; Jia, M.; Xu, T.; Pan, C.; Qi, X.; Zhao, M. Lightweight SM-YOLOv5 Tomato Fruit Detection Algorithm for Plant Factory. *Sensors* **2023**, *23*, 3336. [CrossRef] [PubMed]
27. Li, F.; Na, X.; Shi, J.; Sun, Q. FM-YOLOv8: Lightweight gesture recognition algorithm. *IET Image Process.* **2024**, *18*, 4023–4031. [CrossRef]
28. Li, H.; Zhu, Q.; Huang, M.; Guo, Y.; Qin, J. Pose estimation of sweet pepper through symmetry axis detection. *Sensors* **2018**, *18*, 3083. [CrossRef] [PubMed]
29. Lehnert, C.; Sa, I.; McCool, C.; Upcroft, B.; Perez, T. Sweet pepper pose detection and grasping for automated crop harvesting. In Proceedings of the 2016 IEEE International Conference on Robotics and Automation (ICRA), Stockholm, Sweden, 16–21 May 2016.
30. Lin, G.; Tang, Y.; Zou, X.; Xiong, J.; Li, J. Guava detection and pose estimation using a low-cost RGB-D sensor in the field. *Sensors* **2019**, *19*, 428. [CrossRef]
31. Zhang, Q.; Gao, G. Grasping model and pose calculation of parallel robot for fruit cluster. *Trans. CSAE* **2019**, *35*, 37–47, (In Chinese with English abstract).
32. Yun, S.; Zhang, Q. A method of recognizing the grapefruit axial orientation by binocular vision. *J. Jiangnan Univ. (Nat. Sci. Ed.)* **2012**, *11*, 33–37.
33. Wang, A.; Chen, H.; Liu, L.; Chen, K.; Lin, Z.; Han, J.; Ding, G. Yolov10: Real-Time end-to-End object detection. *arXiv* **2024**, arXiv:2405.14458.
34. Khanam, R.; Hussain, M. YOLOv11: An overview of the key architectural enhancements. *arXiv* **2024**, arXiv:2410.17725.
35. Howard, A.G.; Zhu, M.; Chen, B.; Kalenichenko, D.; Wang, W. MobileNets: Efficient convolutional neural networks for mobile vision applications. *arXiv* **2017**, arXiv:1704.04861.